The Journal of Physical Chemistry A

 VOLUME 102, NUMBER 2, JANUARY 8, 1998

LETTERS

Ab Initio Model Study of the Mechanism of Chlorine Nitrate Hydrolysis on Ice

Roberto Bianco and James T. Hynes*

Department of Chemistry and Biochemistry, University of Colorado, Boulder, Colorado 80309-0215

Received: February 6, 1997; In Final Form: November 11, 1997[⊗]

The hydrolysis of chlorine nitrate $ClONO_2 + H_2O \rightarrow HOCl + HNO_3$ on a type-II polar stratospheric cloud ice aerosol is modeled via the $ClONO_2 \cdot (H_2O)_3$ reaction system at the HF/6-31+G** level of theory with microsolvation by three additional STO-3G waters, and with electron correlation accounted for at the MP2 level. The calculations suggest a fast reaction, consistent with experimental observations, and portray a transition state that involves a nucleophilic attack of a water molecule on chlorine concerted with proton transfer from the attacking water to the ice lattice. The results also give insight on the observed slow desorption of the produced HOCl and indicate a source of rate suppression on sulfate and nitrate containing type-I polar stratospheric cloud ice aerosols.

I. Introduction

The heterogeneous chemistry of $ClONO_2$ and HCl in polar stratospheric clouds (PSCs) has been recognized as a major contributor to ozone depletion in the Antarctic stratosphere.[1] In the Antarctic winter, the PSC ice aerosols are the reaction site of the transformation of $ClONO_2$ and HCl to Cl_2 and HOCl, both photolyzed in the spring to produce Cl atoms, largely responsible for the catalytic depletion of ozone.[1−5] The reaction of $ClONO_2$ with HCl on PSC aerosols has been the focus of several experimental studies,[5−17] some of which indicate the possibility of the two-step mechanism[13−16]

$$ClONO_2 + H_2O \xrightarrow{ice} HOCl + HNO_3 \qquad (I.1)$$

$$HOCl + HCl \xrightarrow{ice} Cl_2 + H_2O \qquad (I.2)$$

as opposed to the direct reaction $ClONO_2 + HCl \xrightarrow{ice} Cl_2 + HNO_3$, at least on water ice. Reaction I.1 itself is of independent interest as a source of HOCl. Experimental work[5−18] has the general conclusion that reaction I.1 proceeds readily on either type-II (water-ice) or water-rich type-I PSCs (containing H_2SO_4 and HNO_3).[19] On the mechanistic side, Hanson[11] has established the $Cl-ONO_2$ bond cleavage on pure $H_2^{18}O$ ice. Further, Sodeau, Horn, Banham, and Koch (SHBK)[15] have proposed that reaction I.1 occurs via the two step mechanism

$$H_2O + ClONO_2 \rightarrow H_2OCl^+NO_3^- \qquad (I.3)$$

$$H_2OCl^+NO_3^- + H_2O \rightarrow H_3O^+ + HOCl + NO_3^- \qquad (I.4)$$

with the nucleophilic attack of a neutral water molecule on Cl, on the basis of IR bands assigned to the reactive intermediate H_2OCl^+ ion (see ref 20 for a review). Some theoretical studies have focused on $ClONO_2$[21] and its water complexes;[22] however, there have been, to our knowledge, no attempts to model in detail the reaction mechanism.[23]

In this Letter, we present model electronic structure calculations to elucidate the mechanism of reaction I.1 on water-ice (type-II PSCs)[5−9,12−14] in the absence of acid catalysis and address the role played by the ice lattice. In our view, an unassisted water molecule is too weak a nucleophile[24] to carry

* Corresponding author. E-mail, hynes@spot.colorado.edu; FAX, +(303) 492 5894.

[⊗] Abstract published in *Advance ACS Abstracts,* December 15, 1997.

S1089-5639(97)00466-0 CCC: $15.00
Published on Web 01/08/1998

TABLE 1. $ClONO_2$ Water Complexes: Structures and Charge Distributions[a]

	$ClONO_2$[b]	C_{Cl}[c]	C_O	R[d]	TS	R_s[e]	P_s	P_s
Cl_1-O_2	1.666	1.674	1.668	1.684	2.136	1.862	2.102	2.381
O_2-N_3	1.372	1.361	1.365	1.348	1.255	1.313	1.268	1.217
N_3-O_4	1.173	1.176	1.178	1.184	1.228	1.199	1.221	1.268
N_3-O_5	1.173	1.176	1.172	1.173	1.191	1.181	1.189	1.190
Cl_1-O_6		2.734		2.596	1.783	2.046	1.817	1.684
O_6-H_7		0.944		0.954	1.256	0.975	1.041	1.770
H_7-O_9				1.911	1.123	1.560	1.345	0.956
O_9-H_{10}				0.952	0.999	0.960	0.976	1.561
$H_{10}-O_{12}$				1.942	1.537	1.681	1.581	0.989
$O_{12}-H_{13}$			0.944	0.946	0.963	0.949	0.957	1.067
$H_{13}-O_4$			2.503	2.207	1.772	1.798	1.778	1.396
H_8-O_6		0.944		0.943	0.948	0.945	0.949	0.947
$H_{11}-O_9$				0.943	0.948	0.943	0.945	0.945
$H_{14}-O_{12}$			0.944	0.943	0.999	0.943	0.943	0.948
$\angle Cl_1O_2N_3$	115.9	116.0	115.8	116.7	121.0	121.7	121.1	121.4
$\angle O_2N_3O_4$	118.6	119.0	118.8	119.0	119.1	118.9	118.9	119.5
$\angle O_2N_3O_5$	110.9	112.0	111.4	112.4	119.2	116.5	118.9	121.9
$\angle O_2Cl_1O_6$		177.0		178.4	179.2	176.2	179.2	179.9
$\angle Cl_1O_6H_7$		123.0		112.1	107.2	106.8	107.9	105.7
$\angle H_7O_6H_8$		107.4		107.4	118.2	109.5	113.8	132.5
$\angle N_3O_4H_{13}$			143.6	156.0	146.1	146.0	146.4	140.8
$O_4H_{13}O_{12}$			155.0	171.0	170.2	169.4	170.3	161.1
$H_{13}O_{12}H_{14}$			107.3	107.1	107.4	107.4	107.3	110.7
$q(Cl_1)$	0.26	0.32	0.27	0.35	0.31	0.30	0.29	0.17
$q(O_2)$	−0.17	−0.18	−0.16	−0.20	−0.34	−0.29	−0.35	−0.32
$q(N_3)$	0.28	0.24	0.29	0.25	0.34	0.31	0.33	0.36
$q(O_4)$	−0.18	−0.20	−0.22	−0.25	−0.46	−0.35	−0.43	−0.56
$q(O_5)$	−0.19	−0.20	−0.19	−0.19	−0.31	−0.26	−0.32	−0.34
$q(O_6)$		−0.74		−0.80	−0.80	−0.76	−0.71	−0.70
$q(H_7)$		0.38		0.47	0.65	0.56	0.63	0.49
$q(H_8)$		0.38		0.37	0.42	0.23	0.24	0.24
$q(O_9)$				−0.84	−0.84	−0.97	−0.99	−0.94
$q(H_{10})$				0.47	0.60	0.52	0.55	0.58
$q(H_{11})$				0.38	0.43	0.24	0.25	0.24
$q(O_{12})$			−0.76	−0.82	−0.90	−0.92	−0.94	−0.79
$q(H_{13})$			0.39	0.44	0.52	0.48	0.50	0.63
$q(H_{14})$			0.37	0.38	0.40	0.24	0.24	0.23

[a] All calculations at the HF/6-31+G** level of theory unless otherwise specified. Bond lengths in Å, angles in deg, Mulliken charges in au. Refer to Figure 2 for structural nomenclature. [b] Isolated $ClONO_2$. [c] $C_{Cl} \equiv H_2O{\cdot}ClONO_2$, $E_{C_{Cl}} = -814.307\,467$ au; $C_O \equiv ClONO_2{\cdot}HOH$, $E_{C_O} = -814.303\,912$ au; $E_{ClONO_2} = -738.268\,890$ au; $E_{H_2O} = -76.031\,231$ au. [d] $ClONO_2{\cdot}(H_2O)_3$ reactant complex (R) and transition state (TS): $E_R = -966.395\,667$ au; $E_{TS} = -966.349\,856$ au. [e] HF/(6-31+G**, STO-3G)//MP2 $ClONO_2{\cdot}(H_2O)_3{\cdot}(H_2O)_3$ approximate reactant complex R_s, transition state TS_s, and product complex P_s (cf. Figure 3); $E_{R_s} = -1193.103\,576$ au, $E_{TS_s} = -1193.099\,003$ au, $E_{P_s} = -1193.104\,534$ au.

out the attack on Cl proposed in reaction I.3. As described within, we propose instead a synergetic role of the ice lattice, where the nucleophilicity of the attacking water is enhanced by a *coupled* proton transfer to a nearby water, to generate a stronger nucleophilic species akin to OH^-. Our results indicate a fast reaction, consistent with experiment. They also suggest an explanation for two further experimental observations: the slow desorption of the HOCl[13] produced in the $ClONO_2$ hydrolysis and the reaction inhibition due to sulfate and/or nitrate anions, present in type-I PSC environments. In section II, we discuss the adsorption of $ClONO_2$ on an ice crystal and propose the model reaction system, for which we present results in section III. Concluding remarks are offered in section IV.

II. $ClONO_2$ on an Ice Crystal

In this section, we consider the adsorption of a $ClONO_2$ molecule on the *basal plane face* (bpf) of an ice crystal—evidently the dominant form of type-II PSCs under stratospheric conditions[25]—with the goal of selecting a model reaction system. All calculations have been carried out at the Hartree Fock (HF)[26] level of theory with the 6-31+G** basis set[27] (unless otherwise specified) by using the quantum chemistry package GAMESS.[28]

Our calculated isolated $ClONO_2$ optimized geometry (see Table 1, first column) is in satisfactory agreement with the accurate calculation by Lee.[21] The $ClONO_2$ molecule is planar, with Cl bearing a partial positive charge due to the strong nitrate group electron attraction. The bpf top bilayer, shown in Figure 1a with adsorbed $ClONO_2$, presents an incoming molecule with a distribution of partially positive hydrogens and electron lone pairs, ideally all perpendicular to the surface. Our chosen arrangement of $ClONO_2$ on the bilayer in Figure 1a can then be rationalized as follows. Consistent with the identifications of the $Cl-ONO_2$ bond cleavage by Hanson[11] and of $H_2O\cdots Cl-ONO_2$ as the lowest energy pair complex by La Manna[22] (see also Table 1, column C_{Cl}), we focus on the coordination of $Cl^{\delta+}$ by a bilayer water oxygen lone pair. The Cl-coordination to the lattice has the water-O, Cl, and the nitrate-O in $H_2O\cdots Cl-ONO_2$ almost collinear because of the sp^3-hybridized Cl three lone pairs, while the $ClONO_2$ planarity promotes hydrogen bonding of the nitrate-O cis to Cl to a water in the same (top) monolayer of the attacking water. The two $ClONO_2$-binding waters are also hydrogen bonded to a third water in the second monolayer and form a network with $ClONO_2$[29] that could allow a synergetic flow of both electrons and protons to assist the reaction.

In particular, the diagram Figure 1b, matching the $ClONO_2$ adsorption site on the bpf, Figure 1a, suggests that the nucleophilic attack of the water-O could be assisted by a proton

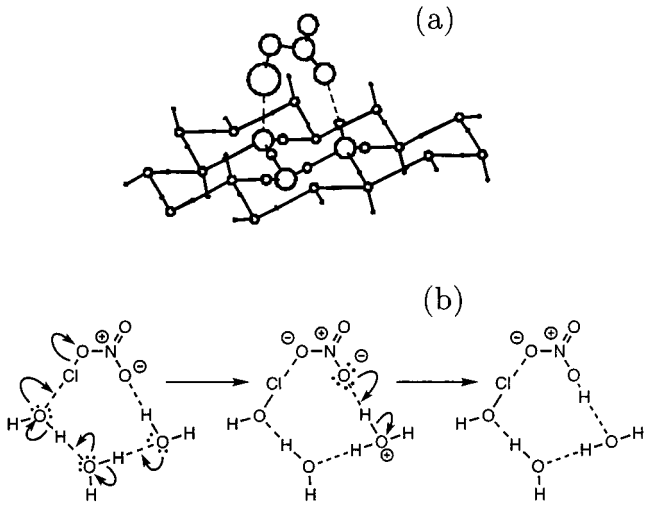

Figure 1. (a) $ClONO_2$ adsorbed on the basal plane face of an ice crystal. The atoms of the core reaction system $ClONO_2 \cdot (H_2O)_3$ are drawn on a larger scale than the rest of the lattice waters. The largest sphere represents Cl. (b) Schematic reaction diagram with the suggested synergetic e^-/H^+ transfers.

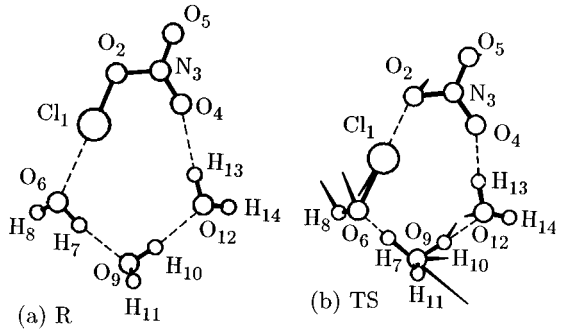

Figure 2. HF/6-31+G** optimized CRS reactant complex (R) and transition state (TS) structures. In both pictures, the atoms O_6, Cl_1, O_2, N_3, O_4, O_5, H_{13}, and O_{12} lay approximately in the plane of the page. TS vibrational mode components in mass-weighted coordinates.

transfer to the next water in the cycle, thus generating a species akin to a hydroxyl anion OH^-, a nucleophile intrinsically stronger than a neutral water molecule.[24] The expected products HOCl and HNO_3 are obtained via electron and proton transfers in the cycle—with HNO_3 possibly dissociated in a polar environment (see section III.d)—and the synergetic charge flow, besides generating an OH^- at the Cl end, also produces a better leaving nitrate group via hydrogen bonding to a lattice water.

The *core reaction system* (CRS) $ClONO_2 \cdot (H_2O)_3$ highlighted in Figure 1a is thus representative of the $ClONO_2$ hydrolysis, since it allows the established nucleophilic attack site, the expected products, and a possible catalytic role of the ice lattice. We now turn to calculations on this CRS to assess the fundamental characteristics of the mechanism.

III. The Core Reaction System $ClONO_2 \cdot (H_2O)_3$

a. Reactant Complex (R). The optimized structure of R is shown in Figure 2a, and its parameters are reported in Table 1, column R. The polarization of $ClONO_2$ in R in the way anticipated in Figure 1b is evident by comparing both its charge distribution and geometry to those of isolated $ClONO_2$, while the ring O−H bonds are longer than the O−H bonds out of the ring and increase in length progressively clockwise from the rightmost water, thus indicating a collective proton drift away from Cl and toward the nitrate group. Further indication of the stabilizing $ClONO_2$/ice synergism are the Cl_1-O_6 and $H_{13}-O_4$ bond lengths, shorter than the corresponding bonds in the $H_2O\cdots Cl-ONO_2$ and $ClON(O)-O\cdots HOH$ complexes (cf. columns C_{Cl} and C_O, respectively, in Table 1).[30]

b. Transition State (TS). To identify the TS, we first located the maximum along the constrained minimum energy path obtained by progressively reducing the Cl_1-O_6 distance in the CRS, starting from R—i.e., forcing the nucleophilic attack—and optimizing all other structural parameters. This preliminary calculation was carried out at the HF/STO-3G[27] level, with the resulting optimized TS geometry used, in turn, as the starting guess for a HF/3-21+G**[27] TS optimization, whose resulting parameters finally provide the initial guess for the HF/6-31+G** optimized TS, the latter displayed in Figure 2b together with its corresponding normal-mode vector components in mass-weighted coordinates. This TS identifies a CRS potential energy surface saddle point characterized by a single imaginary frequency ($715i$ cm^{-1}, unscaled), and it shows the *concerted character of the nucleophilic attack along* the $O_6-Cl_1-O_2$ *axis with the* H_7 *proton transfer from* O_6 to O_9. The Cl_1-O_6 distance is considerably shorter than in R and relatively close to the corresponding equilibrium bond length in isolated HO−Cl (1.667 Å, calculated), whereas O_2 is considerably farther from Cl_1 than in R. In the model ice lattice, the transferring H_7 is closer to the acceptor O_9 than to the donor O_6, while both O_9-H_{10} and $H_{11}-O_9$ are longer than in R, thus suggesting a H_3O^+ ion. To summarize, the TS involves the nucleophilic attack on Cl *concerted* with proton transfer from the attacking water to the model ice lattice. This critical combination is a transition-state feature common to *all* the basis sets used.

c. Intrinsic Reaction Coordinate (IRC) Path. The calculated HF IRC path[31] (not displayed) from the TS toward the products involves a sequence of three proton transfers, to produce energetically favorable HOCl and molecular HNO_3, $\Delta E \simeq -8$ kcal/mol, as anticipated by Figure 1b; this is in contrast to the gas-phase result $\Delta H_f(298) = 2 \pm 3$ kcal/mol.[32] However, the calculated energy barrier $E(TS) - E(R) \simeq 29$ kcal/mol is too large for the CRS to be quantitatively representative of the real reaction on ice,[33] with estimated experimental barrier height of 6.6 kcal/mol.[34] We therefore need to consider further solvation effects.

d. Microsolvation Effects. We have estimated the effect of a larger model ice lattice on the barrier height by microsolvating the three waters in the CRS Figure 2a along the HF IRC path, although without reoptimizing its geometry.[35] Three solvating STO-3G waters have each been positioned at a fixed O−O distance of 2.75 Å (typical of hexagonal ice[36]) from each CRS water, hydrogen bonded to H_8, H_{11}, and H_{14};[37] the corresponding O−H···O angles have been fixed at 180° (see Figure 3 inset). Electron correlation has been accounted for via second-order Møller−Plesset (MP2) perturbation theory.[38]

The MP2 microsolvated reaction path is shown in Figure 3 with associated parameters reported in Table 1. Starting from negative values of the reaction coordinate R_C, we have initially the reactant complex R_s. TS_s corresponds to the concerted S_N2/PT (second-order nucleophilic substitution/proton transfer) approximate transition state, whose associated (cubic spline interpolated) energy is about 3 kcal/mol higher than that of R_s. At PT_2, the first PT has been completed, with the hydronium ion solvated by the ice lattice, and the reaction system preparing for the second PT, completed at P_s, with H_3O^+ forming an ion pair with NO_3^-. The $PT_2 \rightarrow P_s$ step proceeds without barrier, presumably due to the energetically favorable formation of the $H_3O^+NO_3^-$ contact ion pair.[39] The produced HOCl can desorb

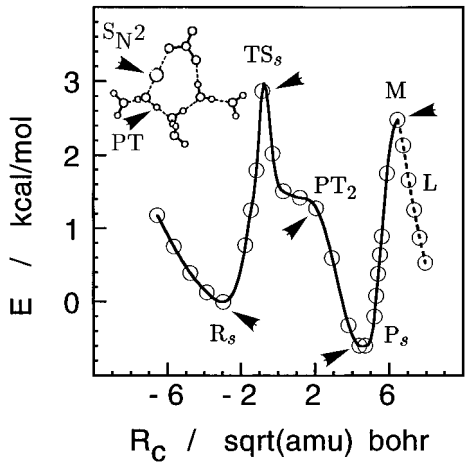

Figure 3. $ClONO_2 \cdot (H_2O)_3 \cdot (H_2O)_3$ HF/(6-31+G**,STO-3G)//MP2 microsolvated reaction path. The structure of the approximate transition state, labeled TS_s, is displayed in the inset.

or diffuse and react with other species, if present.[40] Structure P_s is reminiscent of the local environment of the NO_3^- ion in the crystal structure of nitric acid trihydrate, known to be ionic, i.e., $H_7O_3^+NO_3^-$;[41] this may be the reason why the final PT to form molecular HNO_3, structure M, involves a sharp rise in energy. (In a separate HF/6-31+G** calculation involving only R_s and TS_s, the addition of a solvating water molecule on O_5 (see Figure 2) further stabilizes TS_s with respect to R_s by ca. 2 kcal/mol: this is a small contribution relative to the solvation of the ring water chain, consistent with the slight variation of the partial charge on O_5 going from R_s to TS_s.) The sudden decrease in energy past M (dashed region L) is an artifact due to the absence of structural lattice constraints: once HNO_3 is formed, the $O_2NO-H\cdots OH_2$ hydrogen bond weakens due to loss of collinearity, thus allowing for the (artificial) geometrical relaxation of the $HOCl/HONO_2$/model lattice system. This feature should disappear in calculations involving the proper constraints for the model lattice. Our calculated reaction path does not provide conclusive evidence for HNO_3 to be either in its ionic or molecular form, although the contact ion pair $H_3O^+NO_3^-$ seems to be energetically more favorable.

IV. Concluding Remarks

The present calculations indicate that the $ClONO_2$ hydrolysis on ice proceeds via the nucleophilic attack at Cl by a lattice water molecule *concerted* with proton transfer. This mechanism involves an active, synergetic role of the ice lattice, which helps to generate both a strong, OH^--like attacking nucleophile via proton transfer and a good leaving NO_3^- group via partial protonation. Calculations including correlation effects at the MP2 level, together with partial microsolvation, yield a reaction barrier of about 3 kcal/mol.

Our results contrast with previous proposals for the mechanism. Hanson[11] has proposed that $ClONO_2$ forms a cycle with a *single* water molecule, coordinated to both Cl and the cis O in the nitrate group. But this structure is energetically unfavorable in view of the fully optimized geometries of the $H_2O\cdots Cl\text{-}ONO_2$ and $ClON(O)\text{-}O_{cis}\cdots HOH$ complexes[42] (cf. Table 1, columns C_C and C_O) and also is not consistent with the geometry of the site on the bpf of an ice crystal (cf. Figure 1).

SHBK's proposal[15] (cf. reactions I.3 and I.4) relies on the assignment of a *sharp* peak at 1650 cm^{-1} in the IR spectrum (≡A) at 180 K of a $ClONO_2/H_2O$ 10:1 mixture to the deformation mode of the H_2OCl^+ ion, *by direct analogy* with a rather *broad* peak at 1750 cm^{-1} in the IR spectrum (≡B) of a N_2O_5/H_2O 1:10 mixture (at the same temperature), assigned to the H_3O^+ deformation; see Figure 2 in ref 15. SHBK do not report the identification of any Cl−O stretch. We would advocate a different interpretation. To this end, we note that *all* the bands present in spectrum A are *also* present in spectrum B, although with different intensities (in particular, both the A and B spectra show the two bands at 1750 and 1650 cm^{-1}, with the former appearing as a shoulder in spectrum A, where the latter is prominent, and vice versa for spectrum B); thus the sample corresponding to spectrum A must contain the same species as spectrum B, namely H_2O, H_3O^+, NO_3^-, and solvated molecular HNO_3, although in different proportions. Consequently, any Cl-containing species must be absent from *both* samples, a scenario consistent with a reaction-produced mixture of H_3O^+, NO_3^-, and HNO_3 and the fast production and desorption of HOCl[43] relative to the time taken to record the IR spectrum.

SHBK[15] interpret the MS detection of Cl-containing species, when the water vapor pressure is increased, as indicating evolution of HOCl from the film, which would be inconsistent with our statement above that spectrum A exhibits no Cl-containing species. However, while the IR detector exclusively monitors the composition of the ice film on the gold foil, the MS detector monitors the composition of the gas phase in the chamber, the latter including species desorbed from both the ice film and other apparatus surfaces—e.g., tungsten posts and steel walls—colder than the resistively heated gold foil (see ref 44 and Figure 6 in ref 45). Thus, since the MS detection of Cl-containing species does not unambiguously identify the origin of these species as the ice film on the gold foil, it is plausible that the $ClONO_2$ excess was adsorbed elsehwere in the chamber and remobilized as HOCl via hydrolysis by the increase in water pressure. With this scenario, our suggested alternate interpretation of the SHBK spectra still stands.

We thus believe that the 1650 cm^{-1} peak in spectrum A should be assigned to solvated molecular HNO_3,[46] and not to H_2OCl^+. Further, while our calculations indicate significant interaction between the model ice lattice and $ClONO_2$, with a marked polarization of the reactant $ClONO_2$ molecule (cf. columns $ClONO_2$ and R_s in Table 1), the proposed $H_2OCl^+NO_3^-$ ion pair of ref 15 is not identifiable in our reactant complex R_s along the MP2 microsolvated reaction path of Figure 3 (cf. Cl_1-O_2 and Cl_1-O_6 in column R_s of Table 1).[47] Furthermore, it is worth noting that the existence of the species $[H_2OX]^+$, X = Cl, Br, was ruled out by Eigen and Kustin[48] in their extensive aqueous solution studies of the halogen hydrolysis reactions $X_2 + H_2O \rightarrow XOH + H^+ + X^-$.

Our microsolvated model also gives insight into two further experimental observations. The relatively slow desorption of HOCl from the HNO_3-contaminated ice surface is known to be due to the relatively large adsorption enthalpy of HOCl on ice and not to a slow $ClONO_2$ hydrolysis.[13] The HOCl molecule produced in the microsolvated model reaction system (see inset in Figure 3) finds itself with both O and H coordinated to the lattice and Cl coordinated to one oxygen of the nitrate group. This suggests that the desorption of HOCl from a *full* lattice could involve the cleavage of *three* hydrogen bonds (ca. 10−15 kcal/mol) and a $HOCl\cdots ONO_2^-$ bond, with a corresponding enthalpy consistent with, and possibly slightly larger than, that for HOCl desorption from water ice of 14 ± 2 kcal/mol.[13] For the $ClONO_2$ hydrolysis at 160 K, Oppliger et al.[12] find that $ClONO_2$ disappearance is not accompanied by HOCl desorption and that HCl does not react with the doped surface. HOCl

desorption occurs, however, when the temperature is increased. These authors interpret the observations at 160 K via the formation of a precursor P of HOCl, assumed to be the $H_2OCl^+ \cdot NO_3^-$ contact ion pair. These results can, however, be accounted for within our mechanistic picture. In particular, at 160 K, in a *nondynamic* surface, the HOCl produced would be expected to be *unreactive* because it would be fully coordinated to the lattice waters and to the NO_3^- present, whose oxygen blocks the Cl site on HOCl from HCl attack (cf. Figure 3). In this view, *fully coordinated* HOCl is the precursor P to *reactive* HOCl. Concomitantly, HCl would not be expected to ionize, thus further preventing reaction with HOCl. In fact, ionization of HCl via incorporation in the lattice requires a dynamic surface,[25] not present at 160 K.[50]

Second, on type-I PSCs (nitric and sulfuric acid hydrates), experiments indicate that reaction I.1 is slower than on type-II PSC.[13] Given the key role of lattice waters as proton acceptors and donors indicated within, we suggest that nitrate and/or sulfate ions, and the associated H_3O^+ ions, at the $ClONO_2$ absorption site would hinder the essential proton transfers and thus dampen the synergetic, catalytic ice−$ClONO_2$ interaction.

The present model will be improved by extending the ice lattice via the explicit inclusion of further water molecules[49] and by considering alternative adsorption sites.[51,52] Further, complete modeling of proton transfer in the ice lattice will require the quantization of the proton motion[39,52] and may indicate ice lattice H/D kinetic isotope effects as a probe of our suggested mechanism. These important—and computationally intensive—developments are currently under way.

Acknowledgment. This work was supported by NSF Grants ATM-9613802 and CHE-9312267 and by CHE-9412767 CAW-FY 6-15-94 for part of the computing time. Acknowledgement is made to the National Center for Atmospheric Research, sponsored by the NSF, for the bulk of the computing time used in this research. We thank D. Hanson, S. George, B. Berland, M. Tolbert, S. Barone, and M. Zondlo for enlightening discussions about experiments on reactions on ice, and B. Gertner, G. Peslherbe, K. Gesshirt, and J. Zhu for useful discussions.

References and Notes

(1) Solomon, S.; Garcia, R. R.; Rowland, F. S.; Wuebbles, D. J. *Nature* **1986**, *321*, 755. Solomon, S. *Rev. Geophys.* **1988**, *26*, 131; *Nature* **1990**, *347*, 347. Crutzen, P. J.; Arnold, F. *Ibid.* **1986**, *324*, 651. McElroy, M. B.; Salawitch, R. J.; Wofsy, S. C. *Geophys. Res. Lett.* **1986**, *13*, 1296. Toon, O. B.; Hamill, P.; Turco, R. P.; Pinto, J. *Ibid.* **1986**, *13*, 1284. Turco, R. P.; Toon, O. B.; Hamill, P. *J. Geophys. Res.* **1989**, *94*, 16493.

(2) Cicerone, R. J. *Science* **1987**, *237*, 35. McElroy, M. B.; Salawitch, R. J.; Wofsy, S. C. *Planet. Space Sci.* **1988**, *36*, 73. Henderson, G. S.; Evans, W. F. J.; McConnell, J. C. *J. Geophys. Res.* **1990**, *95*, 1899. World Meteorological Organization (WMO). *Scientific Assessment of Stratospheric Ozone: 1989*; Report No. 20; Global Ozone Research and Monitoring Project: Geneva, 1990. Wayne, R. P. *Chemistry of Atmospheres*, 2nd ed.; Oxford University Press: New York, 1991; p 126.

(3) Wennberg, P. O.; et al. *Science* **1994**, *266*, 398.

(4) Molina, M. J.; Rowland, F. S. *Nature* **1974**, *249*, 810.

(5) Molina, M. J.; Tso, T. L.; Molina, L. T.; Wang, F. C. Y. *Science* **1987**, *238*, 1253.

(6) Chu, L. T.; Leu, M.-T.; Keyser, L. F. *J. Phys. Chem.* **1993**, *97*, 12798. Leu, M.-T.; Moore, S. B.; Keyser, L. F. *Ibid.* **1991**, *95*, 7763.

(7) Tolbert, M. A.; Rossi, M. J.; Malhotra, R.; Golden, D. M. *Science* **1987**, *238*, 1258.

(8) Leu, M.-T. *Geophys. Res. Lett.* **1988**, *15*, 17.

(9) Hanson, D. R.; Ravishankara, A. R. *J. Geophys. Res.* **1991**, *96*, 5081.

(10) Barone, S. B.; Zondlo, M. A.; Tolbert, M. A., *J. Phys. Chem. A* **1997**, *101*, 8643.

(11) Hanson, D. R. *J. Phys. Chem.* **1995**, *99*, 13059.

(12) Oppliger, R.; Allanic, A.; Rossi, M. J. *J. Phys. Chem. A* **1997**, *101*, 1903.

(13) Hanson, D. R.; Ravishankara, A. R. *J. Phys. Chem.* **1992**, *96*, 2682.

(14) Abbatt, J. P. D.; Molina, M. J. *J. Phys. Chem.* **1992**, *96*, 7674.

(15) Sodeau, J. R.; Horn, A. B.; Banham, S. F.; Koch, T. G. *J. Phys. Chem.* **1995**, *99*, 6258.

(16) Banham, S. F.; Horn, A. B.; Koch, T. G.; Sodeau, J. R. *Faraday Discuss.* **1995**, *100*, 321.

(17) For recent reviews, see: Worsnop, D. R.; Kolb, C. E.; Zaniser, M. S.; Davidovits, P.; Keyser, L. F.; Leu, M.-T.; Molina, M. J.; Hanson, D. R.; Ravishankara, A. R.; Williams, L. R.; Tolbert, M. A. In *Progress and problems in Atmospheric Chemistry*; Barker, J. R., ed.; Advanced Series in Physical Chemistry 3; World Scientific: Singapore 1995; Chapter 18 and Molina, M. J.; Molina, L. T.; Golden, D. M. *J. Phys. Chem.* **1996**, *100*, 12888.

(18) For experiments on related systems, see e.g.: (a) Nelson, C. M.; Okumura, M. *J. Phys. Chem.* **1992**, *96*, 6112. (b) Schindler, Th.; Berg, Ch.; Niedner-Schatteburg, G.; Bondybey, V. E. *J. Chem. Phys.* **1996**, *104*, 3998. A mechanistic picture is given here of nucleophilic attack by a *preexisting* OH^- involving proton transfer in a negatively charged water cluster. It is to be distinguished from the mechanism described in the text for a neutral system. (c) Robinson, G. N.; Worsnop, D. R.; Jayne, J. T.; Kolb, C. E.; Davidovits, P. *J. Geophys. Res.* **1997**, *102*, 3583.

(19) See e.g. Tolbert, M. A. *Science* **1994**, *264*, 527. Toon, O. B.; Tolbert, M. A. *Nature* **1995**, *375*, 218 and references therein.

(20) Koch, T. G.; Banham, S. F.; Sodeau, J. R.; Horn, A. B.; McCoustra, M. R. S.; Chesters, M. A. *J. Geophys. Res.* **1997**, *102*, 1513.

(21) Lee, T. J. *J. Phys. Chem.* **1995**, *99*, 1943.

(22) La Manna, G. *J. Mol. Struct.: THEOCHEM* **1994**, *309*, 31. See also: Ying, L. and Zhao, X. *J. Phys. Chem. A* **1997**, *101*, 6807.

(23) In ref 20, a HOMO/LUMO analysis of $H_2O \cdot ClONO_2$ is given, but this gives no indication of any barrier height and does not include any further water molecules.

(24) March, J. *Advanced Organic Chemistry*, 4th ed.; Wiley: New York, 1992; p 653.

(25) Gertner, B. J.; Hynes, J. T. *Science* **1996**, *271*, 1563.

(26) Roothaan, C. C. J. *Rev. Mod. Phys.* **1951**, *23*, 69.

(27) Poirier, R.; Kari, R.; Csizmadia, I. G. *Handbook of Gaussian Basis Sets*; Elsevier: Amsterdam, 1985. We used the polarization ("*") exponents 1.1 (H), 0.8 (O,N), and 0.75 (Cl), and the diffusion ("+") exponents 0.0845 (O), 0.0639 (N), and 0.0483 (Cl).

(28) Schmidt, M. W.; Baldridge, K. K.; Boatz, J. A.; Elbert, S. T.; Gordon, M. S.; Jensen, J. J.; Koseki, S.; Matsunaga, N.; Nguyen, K. A.; Su, S.; Windus, T. L.; Dupuis, M.; Montgomery, J. A. *J. Comput. Chem.* **1993**, *14*, 1347.

(29) A cyclic arrangement including a hydrogen-bonded network has arisen in previous calculations on different reaction systems. See, e.g.: Morokuma, K.; Muguruma, C. *J. Am. Chem. Soc.* **1994**, *116*, 10316. Garrett, B. C.; Melius, C. F. In *Theoretical and Computational Models of Organic Chemistry*; Formosinho, S. J., et al., Eds.; Kluwer: Dordrecht, 1991; p 35.

(30) The complex in Table 1, column C_O, is ∼2 kcal/mol higher in energy than the lowest energy $H_2O\cdots Cl\text{-}ONO_2$ complex, column C_{Cl}. In a separate calculation, we have found that the HF/6-31+G** optimized geometry of the $ClO(O)(O)N\cdots OH_2$ complex, with a water lone pair coordinated to $N^{\delta+}$ ($E = -814.305\,695$ au, $Cl_1-O_2 = 1.664$ Å, $O_2-N_3 = 1.367$ Å, $N_3-O_4 = 1.173$ Å, $N_3-O_5 = 1.174$ Å, $N_3-O_6 = 2.880$ Å, O_6-H_7, $O_6-H_8 = 0.944$ Å, and with N_3-O_6 essentially perpendicular to the $O_4-N_3-O_5$ plane) is only ∼ 1 kcal/mol higher in energy than the most stable $H_2O\cdots Cl-ONO_2$ complex. The N-coordination would assist the O_2-N_3 bond cleavage in the acid-catalyzed $ClONO_2$ hydrolysis (see, e.g.: Lee, T. J.; Rice, J. E. *J. Phys. Chem.* **1993**, *97*, 6637. Reference 18a. Van Doren, J. M.; Viggiano, A. A.; Morris, R. A. *J. Am. Chem. Soc.* **1994**, *116*, 6957.

(31) Fukui, K. *J. Phys. Chem.* **1970**, *23*, 4161; *Acc. Chem. Res.* **1981**, *14*, 363.

(32) Calculated from the data in Appendix 1, p 194, of: *Chemical Kinetics and Photochemical Data for Use in Stratospheric Modelling*; JPL Publ. 94−26; Pasadena, CA, 1994.

(33) Inclusion of electron correlation at the HF/6-31+G**//MP2 level for the frozen R and TS geometries yielded a barrier height ∼20 kcal/mol.

(34) Tabazadeh, A.; Turco, R. P. *J. Geophys. Res.* **1993**, *98*, 12727. See also: Henson, B. F.; Wilson, K. R.; Robinson, J. M. *Geophys. Res. Lett.* **1996**, *23*, 1021 and references therein.

(35) Our calculations do not account for the geometrical constraints due to a full lattice. This is apparent from Figure 2, where the TS ring shrinking is noticeable, especially in the lower part, compared to the R ring. Thus, one should expect a few kcal/mol barrier height increase due to these full lattice constraints (although this might in turn be offset by barrier lowering via solvation by further waters).

(36) See, e.g.: Davidson, E. R.; Morokuma, K. *J. Chem. Phys.* **1984**, *81*, 3741.

(37) The solvating waters arrangement is biased in favor of the full stabilization of a H_3O^+ ion in the water portion of the CRS.

(38) Møller, C.; Plesset, M. S. *Phys. Rev.* **1934**, *46*, 618.

(39) Ando, K.; Hynes, J. T. In *Structure and Reactivity in Aqueous Solution: Characterization of Chemical and Biological Systems*; Cramer,

C. J., Truhlar, D. G., Eds.; American Chemical Society: Washington, DC, 1994; p 143; *J. Mol. Liq.* **1995**, *64*, 25; *J. Phys. Chem.*, in press.

(40) For recent work on reactions on ice involving HOCl, see e.g.: Abbatt, J. P. D.; Nowak, J. B. *J. Phys. Chem. A* **1997**, *101*, 2131. Donaldson, D. J.; Ravishankara, A. R.; Hanson, D. R. *Ibid.* **1997**, *101*, 4717.

(41) See Figure 3 in: Taesler, I.; Daleplane, R. G.; Olovsson, I. *Acta. Crystallogr.* **1975**, *B31*, 1489. In our case, NO_3^- is bound to the surface by a strong hydrogen bond to a $H_3O^+(H_2O)_2$ group, like in crystalline nitric acid trihydrate (NAT), and is coordinated to $Cl^{\delta+}$ of HOCl via O_2 (see Figure 2), a bond stronger than the hydrogen bond of nitrate group oxygen to a water (see Table 1, columns C_{Cl} and C_O). Thus, compared to crystalline NAT, instead of three hydrogen bonds, one on one oxygen and two on another oxygen of the nitrate group, we have one Cl···O bond, approximately as strong as two hydrogen bonds.

(42) Similar geometries were reported in ref 22 for the partial optimization of these complexes. Very recently, Akhmatskaya et al. (*J. Chem. Soc., Faraday Trans.* **1997**, *93*, 2775) have found that the reaction barrier for the cyclic $ClONO_2 \cdot H_2O$ complex treated quantum chemically and solvated by 10 additional classical waters is 31.7 kcal/mol, thus ruling out this reaction pathway.

(43) A recent experiment shows that the $ClONO_2$ hydrolysis is very efficient upon $ClONO_2$ deposition on an ice surface in the temperature range 75−140 K (Berland, B.; Tolbert, M.; George, S. *J. Phys. Chem. A*, in press).

(44) Horn, A. B.; Koch, T. G.; Chesters, M. A.; McCoustra, M. R. S.; Sodeau, J. R. *J. Phys. Chem.* **1994**, *98*, 946.

(45) McCoustra, M. R. S.; Horn, A. B. *Chem. Soc. Rev.* **1994**, *23*, 195.

(46) G. Ritzhaupt and J. P. Devlin (*J. Phys. Chem.* **1991**, *95*, 90) have found that monohydrated HNO_3 at 80 K is mostly undissociated at the surface of ice, whereas trihydrated HNO_3 is mostly present as solvated nitrate and hydronium ions; the band near 1650 cm^{-1} in Figures 1 and 2 of this reference is an important component of the IR signature of un-ionized HNO_3 in low-temperature HNO_3/H_2O mixtures.

(47) J. P. Francisco and S. P. Sander (*J. Chem. Phys.* **1995**, *102*, 9615) have calculated at the MP2/6-31G(d) level the Cl−O distance in isolated H_2OCl^+ to be 1.758 Å, far shorter than the 2.046 Å we report in Table 1, column R_s.

(48) Eigen, M.; Kustin, K. *J. Am. Chem. Soc.* **1962**, *84*, 1355.

(49) Bianco, R.; Hynes, J. T., work in progress.

(50) Haynes, D. R.; Tro, N. J.; George, S. M., *J. Phys. Chem.* **1992**, *96*, 8502.

(51) The local structure of the ice surface has a strong influence on the absorption of molecular species; see, e.g.: Graham, J. D.; Roberts, J. T. *J. Phys. Chem.* **1994**, *98*, 5974. Schaff, J. E.; Roberts, J. T. *Ibid.* **1994**, *98*, 6900. Devlin, J. P.; Buch, V. *Ibid.* **1995**, *99*, 16534. Buch, V.; Delzeit, L.; Blackledge, C.; Devlin, J. P. *Ibid.* **1996**, *100*, 3732.

(52) Gertner, B. J.; Hynes, J. T., in preparation.